NEOPLASIA
www.neoplasia.com

Volume 14 Number 7 July 2012 pp. 600–611 600

Molecular Subtyping of Primary Prostate Cancer Reveals Specific and Shared Target Genes of Different ETS Rearrangements[1,2]

Paula Paulo[*,†,‡,§], Franclim R. Ribeiro[*,†,‡,§], Joana Santos[*,†], Diana Mesquita[*,†], Mafalda Almeida[*,¶], João D. Barros-Silva[*,†], Harri Itkonen[#], Rui Henrique[¶,,††], Carmen Jerónimo[*,¶,††], Anita Sveen[‡,§], Ian G. Mills[‡,#,‡‡], Rolf I. Skotheim[‡,§], Ragnhild A. Lothe[‡,§] and Manuel R. Teixeira[*,†,§,††]**

*Department of Genetics, Portuguese Oncology Institute, Porto, Portugal; †Group of Cancer Genetics, Research Centre of the Portuguese Oncology Institute, Porto, Portugal; ‡Department of Cancer Prevention, Institute for Cancer Research, Oslo University Hospital, Oslo, Norway; §Centre for Cancer Biomedicine, University of Oslo, Oslo, Norway; ¶Group of Cancer Epigenetics, Research Centre of the Portuguese Oncology Institute, Porto, Portugal; #Centre for Molecular Medicine Norway, Nordic European Molecular Biology Laboratory Partnership, Biotechnology Centre, University of Oslo, Oslo, Norway; **Department of Pathology, Portuguese Oncology Institute, Porto, Portugal; ††Institute of Biomedical Sciences Abel Salazar, University of Porto, Porto, Portugal; ‡‡Department of Urology, Oslo University Hospital, Oslo, Norway

Abstract

This work aimed to evaluate whether ETS transcription factors frequently involved in rearrangements in prostate carcinomas (PCa), namely ERG and ETV1, regulate specific or shared target genes. We performed differential expression analysis on nine normal prostate tissues and 50 PCa enriched for different ETS rearrangements using exon-level expression microarrays, followed by *in vitro* validation using cell line models. We found specific deregulation of 57 genes in *ERG*-positive PCa and 15 genes in *ETV1*-positive PCa, whereas deregulation of 27 genes was shared in both tumor subtypes. We further showed that the expression of seven tumor-associated *ERG* target genes (*PLA1A*, *CACNA1D*, *ATP8A2*, *HLA-DMB*, *PDE3B*, *TDRD1*, and *TMBIM1*) and two tumor-associated *ETV1* target genes (*FKBP10* and *GLYATL2*) was significantly affected by specific ETS silencing in VCaP and LNCaP cell line models, respectively,

Abbreviations: AR, androgen receptor; DAC, 5-aza-2′deoxycytidine; NPT, normal prostate tissue; PCA, principal components analysis; PCa, prostate carcinoma; qMSP, quantitative methylation-specific PCR; qRT-PCR, quantitative real-time polymerase chain reaction; shRNA, short hairpin RNA; siRNA, small interfering RNA; TSA, Trichostatin A

Address all correspondence to: Manuel R. Teixeira, MD, PhD, Department of Genetics, Portuguese Oncology Institute – Porto, Rua Dr. António Bernardino de Almeida, 4200-072 Porto, Portugal. E-mail: manuel.teixeira@ipoporto.min-saude.pt

[1]This work was supported by research grant PTDC/SAU/OBD/70543/2006 awarded by Fundação para a Ciência e a Tecnologia (FCT) and by research grant CI-IPOP-8-2008 funded by the Portuguese Oncology Institute, Porto (M.T.). P.P. (SFRH/BD/27669/2006), F.R.R. (SFRH/BPD/26492/2006), J.S. (SFRH/BD/73964/2010), and J.D.B.S. (SFRH/BD/46574/2008) are research fellows from FCT. D.M. is a research fellow from Liga Portuguesa Contra o Cancro, Núcleo Regional do Norte (M.T.). A.S. has a PhD grant from the Research Council at Rikshospitalet-Radiumhospitalet Health Enterprise (R.A.L.). The study is also supported by grants from the Norwegian Cancer Society (PR-2007-0166 to R.I.S. and PR-2006-0442 to R.A.L.). H.I. is funded by an Early Stage Researcher fellowship as part of the EU FP7 Marie Curie Integrated Training Network, PRO-NEST (Prostate Research Organizations – Network Early Stage Training). I.G.M. is supported by funding from the Norwegian Research Council, Helse Sor-Ost and the University of Oslo through the Centre for Molecular Medicine (Norway), which is the part of the Nordic EMBL (European Molecular Biology Laboratory) partnership. I.G.M. is also supported by the Norwegian Cancer Society and by EU FP7 funding. I.G.M. holds a visiting scientist position with Cancer Research UK through the Cambridge Research Institute and a Senior Visiting Research Fellowship with Cambridge University through the Department of Oncology. The authors declare no conflict of interest.
[2]This article refers to supplementary materials, which are designated by Tables W1 to W5 and Figure W1 and are available online at www.neoplasia.com.
Received 29 March 2012; Revised 5 June 2012; Accepted 6 June 2012

DOI 10.1593/neo.12600

whereas the expression of three candidate *ERG* and *ETV1* shared targets (*GRPR*, *KCNH8*, and *TMEM45B*) was significantly affected by silencing of either ETS. Interestingly, we demonstrate that the expression of *TDRD1*, the topmost overexpressed gene of our list of *ERG*-specific candidate targets, is inversely correlated with the methylation levels of a CpG island found at −66 bp of the transcription start site in PCa and that *TDRD1* expression is regulated by direct binding of ERG to the CpG island in VCaP cells. We conclude that ETS transcription factors regulate specific and shared target genes and that *TDRD1*, *FKBP10*, and *GRPR* are promising therapeutic targets and can serve as diagnostic markers for molecular subtypes of PCa harboring specific fusion gene rearrangements.

Neoplasia (2012) 14, 600–611

Introduction

Genomic rearrangements involving five members of the ETS family of transcription factors have been found in prostate carcinomas (PCa). Rearrangements of *ERG* and *ETV1* were first described by Tomlins et al. [1] and are found in approximately 50% and 5% to 10% of PCa, respectively [2,3]. Rearrangements of *ETV4* and *ETV5* were later identified in a small proportion of PCa, representing less than 5% of all rearranged cases [4–7]. Recently, we identified *FLI1* as the fifth member of the ETS family of transcription factors involved in gene fusions in PCa, being fused to the *SLC45A3* gene [8].

The products of specific chimeric genes could be ideal therapy targets, but the nuclear localization of the aberrant ETS proteins makes them a difficult therapy target *in vivo* [9]. Therefore, it is important to characterize in detail the downstream molecular targets of each of the aberrant transcription factors, not only to understand the deregulated signaling pathways but also because some of them may turn out to be more amenable to targeted therapy. *In vitro* studies revealed that *ERG* activates plasminogen and Wnt pathways to promote degradation of the extracellular matrix and decrease cell adhesion, but very few genes have been validated as direct *ERG* targets [10–12]. Because *ETV1* rearrangements are considerably less frequent than those of *ERG*, reports focusing on the oncogenic effectors of *ETV1* overexpression are scarce and not based in the expression profile observed in *ETV1* rearrangement-positive tumors, with some *in vitro* and *in vivo* models linking overexpression of *ETV1* with the invasion potential of cancer cells by activation of matrix metalloproteinases and integrins [13–15].

Despite the apparently overlapping oncogenic potential of *ERG* and *ETV1* gene fusions, it has not been established whether different ETS transcription factors have shared or specific downstream targets. We addressed this issue by using exon-level expression arrays in a series of 50 PCa enriched for different ETS rearrangements and validated the findings using *in vitro* cell line models.

Materials and Methods

Prostate Tissue Samples

We used a series of 50 tumor samples selected from a consecutive series of 200 clinically localized PCa that were previously typed for ETS rearrangements [8]. The 50 prostatectomy samples were selected to represent the various molecular subtypes of PCa, namely 21 samples with *ERG* rearrangement, 13 samples with *ETV1* rearrangement, 2 samples with other ETS rearrangements (one with *ETV4* and one with *ETV5* rearrangements), and 14 samples without known ETS rearrangement. For control purposes, nine normal prostate tissues (NPTs) were collected from cystoprostatectomy specimens of bladder cancer patients. This study was approved by the institutional review board, and informed consent was obtained from all subjects.

Prostate Cell Lines

VCaP and PNT2 cells were acquired from the European Collection of Cell Cultures (Sigma-Aldrich, St Louis, MO). LNCaP, PC3, and DU145 cells were acquired from the German Resource Centre for Biological Material (DSMZ, Braunschweig, Germany). 22Rv1 cells were kindly provided by Dr David Sidransky from the Johns Hopkins University School of Medicine. The virus packaging Retro-Pack PT67 cell line was acquired from Clontech Laboratories, Inc (Saint-Germain-en-Laye, France). All prostate cell lines were cultured under the recommended conditions, being karyotyped by G banding for validation purposes and tested for *Mycoplasma* spp. contamination (PCR Mycoplasma Detection Set; Clontech Laboratories). After transfection, cells were grown in medium supplemented with G418 (300 μg/ml; GIBCO by Life Technologies, Carlsbad, CA) or puromycin (5 μg/ml, Clontech Laboratories), as appropriate.

Gene Expression Microarrays

RNA was extracted from tissue samples using TRIzol (Invitrogen by Life Technologies, Carlsbad, CA), as previously described [8], and 1 μg of RNA was processed into complementary DNA (cDNA) and hybridized to GeneChip Human Exon 1.0 ST arrays, following the manufacturer's recommendations. The Affymetrix Expression Console v1.1 software was used to obtain gene-level RMA-normalized expression values for the core probe sets only. We used analysis of variance in Partek Genomics Suite 6.4 (Partek, Inc, St Louis, MO) to identify differentially expressed genes among the different sample groups. The two PCa with *ETV4* and *ETV5* rearrangements were not included in this analysis. Specific *ERG* target genes were identified from genes differentially expressed between each of the three group comparisons: NPT *versus ERG*-positive PCa, ETS-negative PCa *versus ERG*-positive PCa and *ETV1*-positive PCa *versus ERG*-positive PCa. To select specific *ETV1* target genes, the same approach was applied comparing NPT *versus ETV1*-positive PCa, ETS-negative PCa *versus ETV1*-positive PCa and *ERG*-positive PCa *versus ETV1*-positive PCa. Targets common to *ERG* and *ETV1* rearrangements were identified from the differentially expressed genes in each of the four group comparisons: NPT *versus ERG*-positive PCa, NPT *versus ETV1*-positive PCa, ETS-negative PCa *versus ERG*-positive PCa and ETS-negative PCa *versus ETV1*-positive PCa. Only differentially expressed genes with a false discovery rate less

than 5% and $P < .02$ between each two-group comparison were retained for further analyses. Principal components analysis (PCA) was performed with Partek Genomics Suite 6.4 and hierarchical clustering with MultiExperiment Viewer 4.6.0. Hierarchical clustering was performed using Spearman rank correlation and average linkage optimized for gene leaf order.

Transient Silencing of ERG *Expression in VCaP Cells*

To induce down-regulation of *ERG* expression in VCaP cells we used small interfering RNAs (siRNAs) as described by others [12]. The SMART-pool siRNA directed to *ERG* (M-003886-01; Dharmacon, Thermo Fisher Scientific, Rockford, IL) and the siCONTROL Non-Targeting RNA (D-001210-01; Dharmacon) were transfected into VCaP cells using Oligofectamine (Invitrogen). After 48 and 72 hours, RNA and protein extractions were performed using the TriplePrep Kit (GE Healthcare, Cleveland, OH). Expression data of VCaP-siERG cells were normalized to VCaP-siCont for each time point.

Generation of Plasmid Constructs for Stable Silencing and De Novo *Overexpression*

To generate constructs for stable silencing of *ETV1*, specific short hairpin RNA (shRNA) sequences were selected and designed using the RNAi Target Sequence Selector and the shRNA Sequence Designer, respectively (both from Clontech Laboratories). shETV1-553 (5′-GATCCGCTCATACACCGAAACCTGATTCAAGA GATCAGGTTTCGGTGTATGAGTTTTTTACGCGTG-3′) and shETV1-1037 (5′-GATCCACAAGAGCCAGGAATGTATTTCAAGAGAATACATTCCTGGCTCTTGTTTTTTTACGCGTG-3′) oligonucleotides were acquired from Sigma-Aldrich, annealed, and cloned into the pSIREN-Retro-Q vector (Clontech Laboratories) at *Bam*HI and *Eco*RI restriction sites, together with the negative control shNeg (Clontech Laboratories). To generate constructs for *de novo* overexpression of *ETV1* and *ERG*, full-length *ETV1* CDS and truncated *ERG* CDS (Δ*ERG* and Δ*ERG*Δ8) were amplified from LNCaP and VCaP cells, respectively, using In-fusion primers (Table W1) and the Phusion Taq DNA polymerase (Finnzymes, Vantaa, Finland). Polymerase chain reaction (PCR) products were cloned into the pMSCVneo vector (Clontech Laboratories) at *Bgl*II and *Eco*RI restriction sites using the In-Fusion Advantage PCR cloning kit (Clontech Laboratories), according to instructions. The pMSCVneo-*ETV1* construct contains the *ETV1* full-length CDS (ENST00000242066), as expected; the pMSCVneo-Δ*ERG* contains the expected CDS derived from the type III *TMPRSS2-ERG* transcript [16] and pMSCVneo-Δ*ERG*Δ8 contains the alternatively spliced transcript lacking 72 bp (exon 8) [17,18].

Stable Silencing of ETV1 *in LNCaP Cells*

To silence the expression of *ETV1* in LNCaP cells, PT67 cells were transfected with each construct and also with the control vector pSIREN-shNeg using the $CaPO_4$-based transfection method, following Clontech's recommendations (protocol no. PT3132-1, version no. PR631543). Transfected cells were selected with puromycin and expanded. LNCaP cells were exposed to viral medium for 8 hours and allowed to recover for 24 hours in regular growth conditions. Stable LNCaP-sh*ETV1* and LNCaP-shNeg populations were obtained with puromycin-selective pressure. Two independent, low *ETV1* expression clones (LNCaP-shETV1-C1 and LNCaP-shETV1-C2) were isolated and used for further analyses.

Stable Overexpression of ETV1 *and Δ*ERG *Isoforms in PNT2 Cells*

For stable expression of the *ETV1* and Δ*ERG* isoforms described, PT67 cells were transfected with pMSCV constructs and with the empty vector pMSCVneo as previously described. Transfected cells were selected with G418 and expanded. Transduction of PNT2 cells was carried out as previously described for LNCaP cells. A control population (PNT2-Neo) and two independent populations showing overexpression of either *ETV1* (PNT2-*ETV1*-A and PNT2-*ETV1*-B) or Δ*ERG* isoforms (PNT2-Δ*ERG*-A, PNT2-Δ*ERG*-B, PNT2-Δ*ERG*Δ8-A and PNT2-Δ*ERG*Δ8-B) were obtained with G418-selective pressure.

In Silico *Selection of Target Genes for Further Validation*

We used the expression data of VCaP, LNCaP, PC3, and DU145 cell lines available from Taylor et al. that can be accessed from the Gene Expression Omnibus (GSE21034) to select the candidate target genes where differential expression was specific of the cell line models harboring ETS rearrangements, taking into consideration the candidate target genes resulting from the microarray analysis of the prostate tumor samples. Using the RMA-normalized signal intensity values, *ERG*-associated genes were selected as those differentially upregulated or downregulated at least 1.5-fold in VCaP cells comparing with the others. Similarly, *ETV1*-associated genes were those differentially upregulated or downregulated at least 1.5-fold in LNCaP cells comparing with the others, and target genes shared by *ERG* and *ETV1* rearrangements were those differentially upregulated or downregulated at least 1.5-fold in VCaP or LNCaP cells comparing with PC3 and DU145 cell lines.

Quantitative Real-time Polymerase Chain Reaction

RNA was extracted from subconfluent cell lines using the RNeasy mini kit (Qiagen, GmbH, Hilden, Germany). cDNA was obtained from 1 μg of RNA using oligo-dT primers and the H-minus RevertAid cDNA synthesis kit (Fermentas, Ontario, Canada), according to the manufacturer's instructions. Expression of target genes was quantified using predeveloped TaqMan assays from Applied Biosystems (Life Technologies, Foster City, CA) (Table W1) and normalized to the expression of the *GUSB* housekeeping gene using the comparative C_t method [19].

Western Blot Analysis

Protein was extracted from subconfluent cells using RIPA lysis buffer in the presence of protease inhibitors (Santa Cruz Biotechnology, Inc, Heidelberg, Germany), and concentration was determined by the BCA protein assay (Thermo Fisher Scientific), following the manufacturer's recommendations. Specific detection of ERG and ETV1 was achieved by incubation with rabbit anti-ERG (1:1000; Epitomics, Burlingame, CA) and mouse anti-ETV1 (1:500; Sigma-Aldrich) monoclonal antibodies, respectively. An anti–β-actin monoclonal antibody (1:8000; Sigma-Aldrich) was used to control protein loading.

Bisulfite Treatment and Quantitative Methylation-Specific PCR of TDRD1

Genomic DNA was extracted from prostate tissues and cell lines using a standard technique comprising digestion with proteinase K (20 mg/ml) in the presence of 10% SDS at 55°C, followed by phenol-chloroform extraction and precipitation with 100% ethanol [20]. In 4 of the 50 PCa samples (1 *ERG*-positive, 1 *ETV1*-positive, and the 2 samples with other ETS rearrangements), it was not possible to obtain DNA. One microgram of DNA was submitted to bisulfite modification

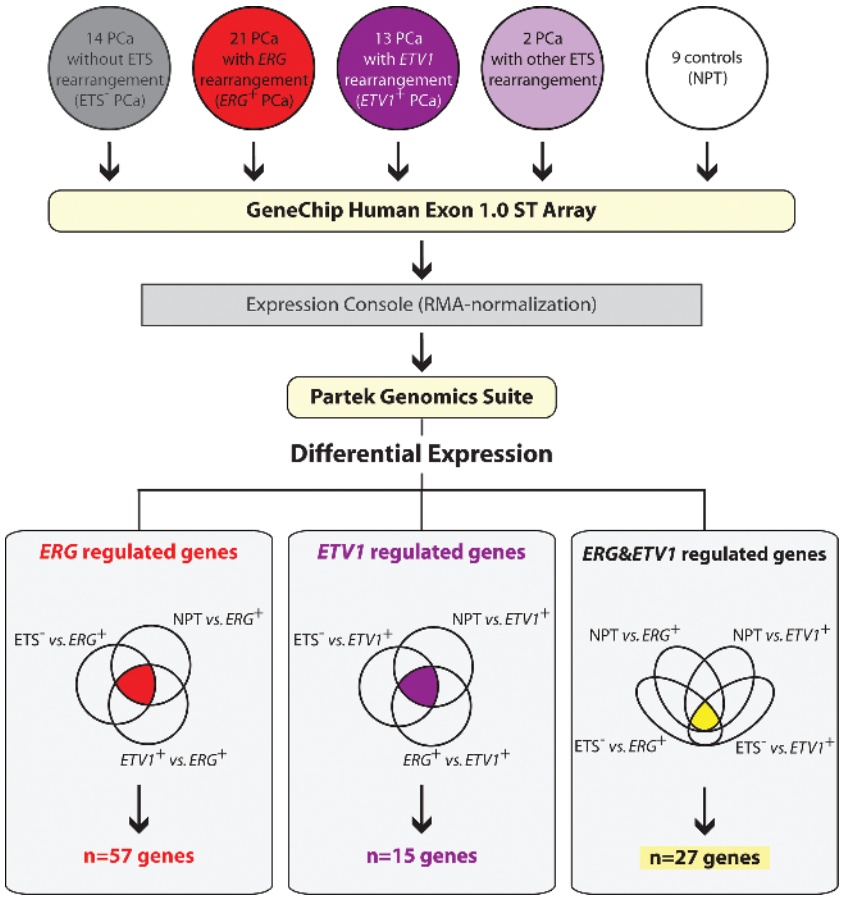

Figure 1. Workflow applied to 9 NPTs and 50 PCa previously characterized for the presence of known ETS rearrangements to identify both specific and shared *ERG* and *ETV1* target genes by differential expression analysis. The two PCa with other ETS rearrangements were not included in Partek Genomics Suite analysis.

using the EZ DNA Methylation Gold Kit (Zymo Research, Orange, CA) following the manufacturer's instructions. Bisulfite-modified DNA was amplified by quantitative methylation-specific PCR (qMSP) using TaqMan technology [21]. Specific *TDRD1* primers and TaqMan probe were designed using the Methyl Primer Express Software v1.0 (Applied Biosystems; Table W1). β-Actin (*ACTB*) was used as an internal reference gene to normalize for DNA input and qMSP reaction was performed as previously described [22]. Methylation levels for each sample were obtained from calibration curves constructed using serial dilutions of bisulfite-modified CpGenome Universal Methylated DNA (Millipore, Billerica, MA). *TDRD1* methylation levels were obtained after normalization to *ACTB*.

Bisulfite Sequencing

To obtain detailed information about the methylation status of CpG sites in the CpG island found in the *TDRD1* promoter, bisulfite-sequencing PCR primers (Table W1) that span the region of interest were tested in bisulfite-modified DNA from VCaP, LNCaP, PC3, DU145, 22Rv1, and PNT2 cells. PCR was performed as previously described [23].

Chromatin Immunoprecipitation and Quantitative PCR

Transcription factor–dependent gene expression is associated with the recruitment of transcription factors to regulatory sequences. This is detected commonly through the use of chromatin immunoprecipitation and, where sites are known or predicted, through quantitative PCR (qPCR) for the bound regions. We used VCaP cells and the rabbit anti-ERG monoclonal antibody (Epitomics) to detect ERG binding to the promoter of candidate target genes. For each immunoprecipitation with the EZ-Magna chromatin immunoprecipitation (ChIP) G kit (Millipore), 2×10^6 cells were used, following the manufacturer's instructions [24,25]. We used two approaches to identify candidate sites within the promoter regions. One approach was to mine the ChIP-Seq data set available from Yu et al. [26] for ERG generated in the VCaP cell line (GSE14092, sample GSM353647). Processed sequencing files were uploaded into the UCSC genome browser and aligned to build hg18. Gene proximal sites were then selected. In addition, we also used *in silico* prediction by uploading promoter sequences into ConSite—http://asp.ii.uib.no:8090/cgi-bin/CONSITE/consite/ [27]. Overall, four promoter regions were analyzed for *TDRD1* (−1207, −3196, −7686, and −8768) and three for *GRPR* (−583, −1386, and −4858), *KCNH8* (−797, −1472, and −3506), and *TMEM45B* (−260, −2847, and −5687). Primers were designed using the Primer3 online software and acquired from Metabion (Martinsried, Germany). Primers for a negative control region were also included to correct for unspecific binding (Table W1) [28]. qPCR was performed using Power SYBR Green (Applied Biosystems), according to the manufacturer's recommendations. Results are shown as a fold enrichment of ERG bound chromatin relative to IgG and corrected to the negative control region [29].

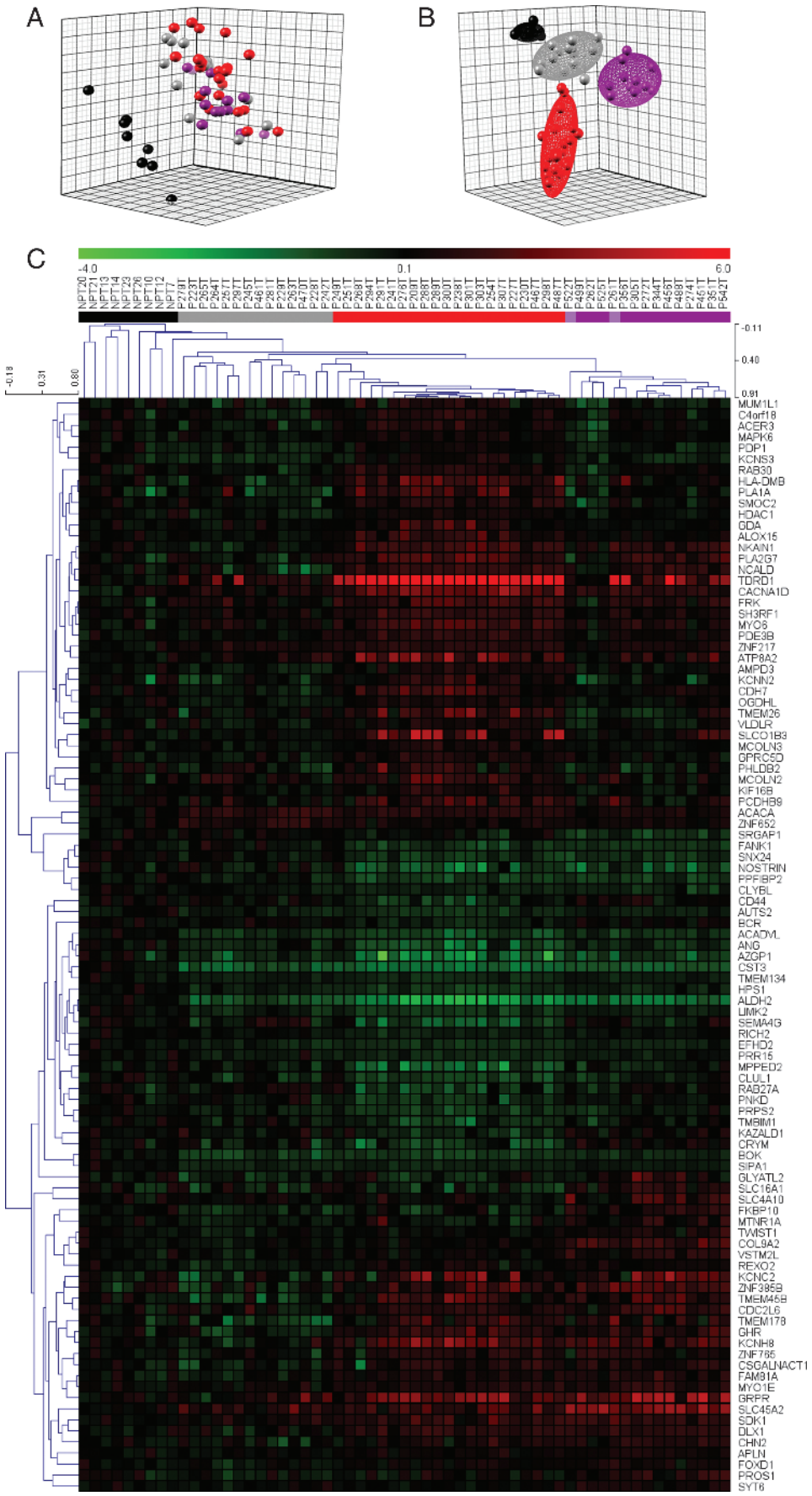
A
B
C
-4.0
0.1
6.0
NPT20
NPT21
NPT13
NPT14
NPT23
NPT26
NPT10
NPT12
NPT7
P279T
P223T
P265T
P264T
P257T
P287T
P245T
P246T
P291T
P259T
P263T
P247T
P228T
P242T
P249T
P251T
P268T
P294T
P281T
P241T
P276T
P209T
P286T
P289T
P299T
P301T
P303T
P254T
P307T
P227T
P230T
P246TT
P298T
P248TT
P522T
P499T
P262T
P525T
P526T
P305T
P272T
P344T
P456T
P488T
P274T
P451T
P351T
P542T
-0.11
0.40
0.91
-0.18
0.31
0.80
MUM1L1
C4orf18
ACER3
MAPK6
PDP1
KCNS3
RAB30
HLA-DMB
PLA1A
SMOC2
HDAC1
GDA
ALOX15
NKAIN1
PLA2G7
NCALD
TDRD1
CACNA1D
FRK
SH3RF1
MYO5
PDE3B
ZNF217
ATP8A2
AMPD3
KCNN2
CDH7
OGDHL
TMEM26
VLDLR
SLCO1B3
MCOLN3
GPRC5D
PHLDB2
MCOLN2
KIF16B
PCDHB9
ACACA
ZNF652
SRGAP1
FANK1
SNX24
NOSTRIN
PPFIBP2
CLYBL
CD44
AUTS2
BCR
ACADVL
ANG
AZGP1
CST3
TMEM134
HPS1
ALDH2
LIMK2
SEMA4G
RICH2
EFHD2
PRR16
MPPED2
CLUL1
RAB27A
PNKD
PRPS2
TMBIM1
KAZALD1
CRYM
BOK
SIPA1
GLYATL2
SLC16A1
SLC4A10
FKBP10
MTNR1A
TWIST1
COL9A2
VSTM2L
REXO2
KCNC2
ZNF385B
TMEM45B
CDC2L6
TMEM178
GHR
KCNH8
ZNF765
CSGALNACT1
FAM81A
MYO1E
GRPR
SLC45A2
SDK1
DLX1
CHN2
APLN
FOXD1
PROS1
SYT6

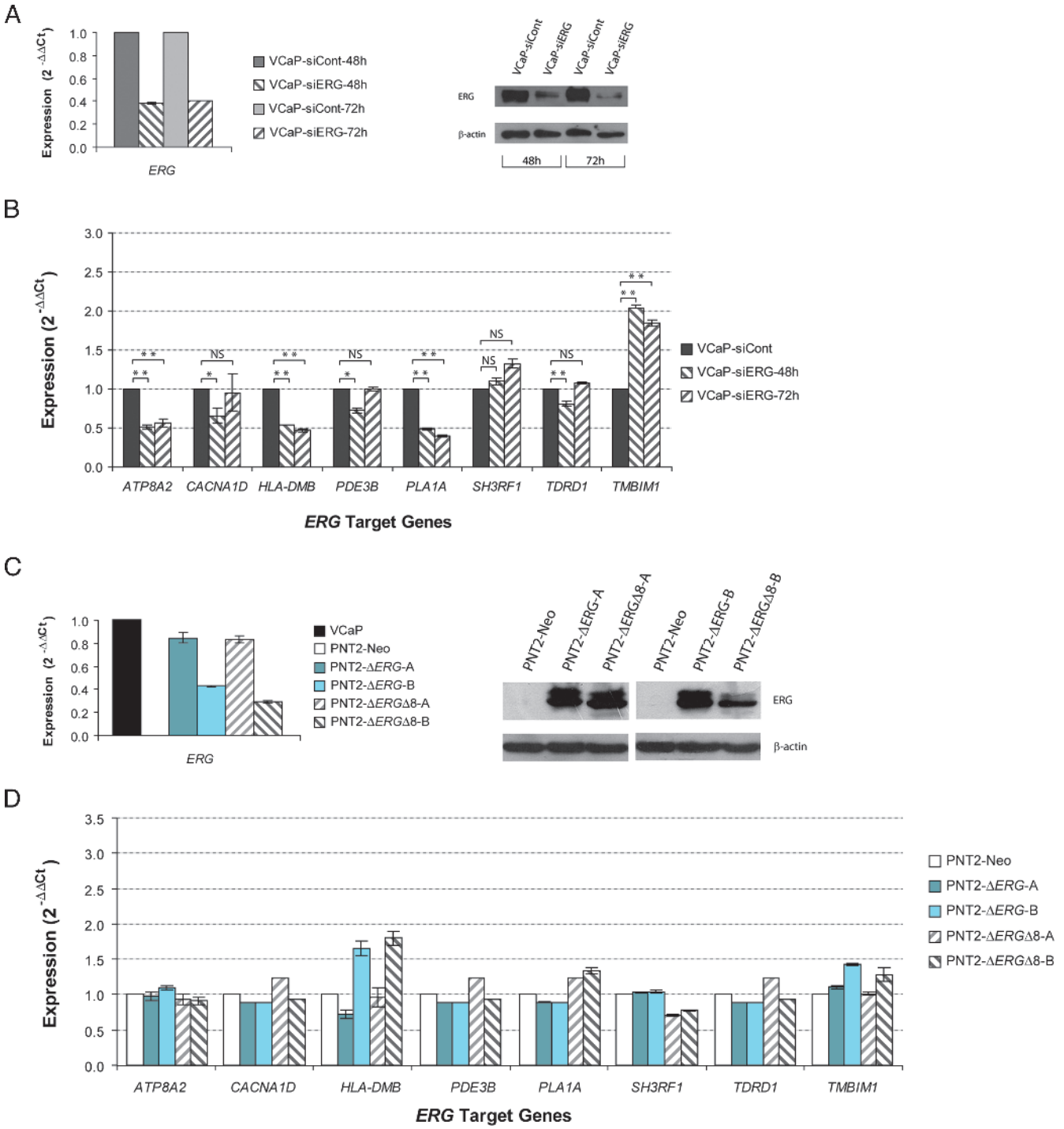

Figure 3. Validation of tumor-associated *ERG* target genes in cell line models. (A) Using siRNAs directed to *ERG*, a significant down-regulation of *ERG* expression was achieved in VCaP cells, as evaluated both by qRT-PCR and by Western blot analyses at 48 and 72 hours after transient transfection. (B) Of the eight tumor-associated *ERG* candidate target genes, seven were significantly deregulated after *ERG* silencing, as evaluated by qRT-PCR. (C) *De novo* expression of two Δ*ERG* isoforms was stably induced in the benign PNT2 prostate cells, as shown both by qRT-PCR and Western blot analyses. (D) *De novo* expression of Δ*ERG* isoforms was not sufficient to induce expression of the tumor-associated ERG target genes in PNT2 cells. *$P < .05$. **$P < .01$. NS indicates not significant ($P > .05$).

Figure 2. PCA and hierarchical clustering of the expression profile obtained for normal controls (NPT) and PCa samples. (A and B) Sample distribution obtained by PCA in Partek Genomics Suite using the full gene expression profile and the 99 gene panel obtained by differential expression analysis, respectively. (C) Hierarchical clustering of the 9 NPT samples and the 50 PCa obtained with the RMA-normalized expression data of the panel of 99 genes selected with Partek's differential expression analysis. The nine NPTs are shown in black, the *ETS*-negative PCa in gray, the *ERG*-positive PCa in red, the *ETV1*-positive PCa in dark purple, and the other *ETS*-positive PCa in light purple.

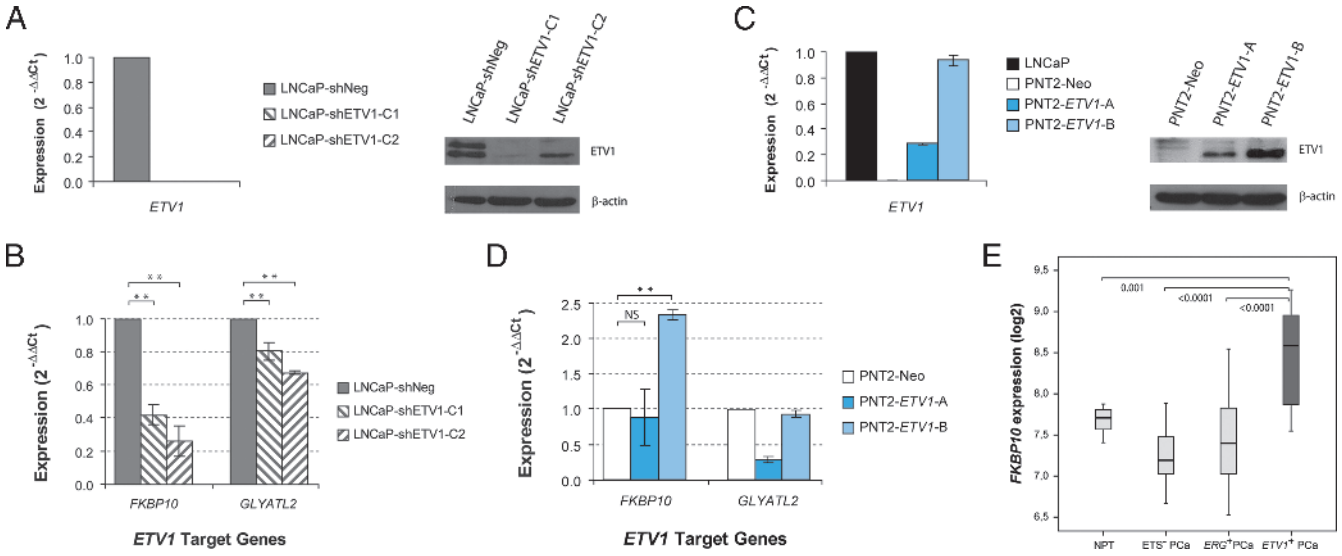

Figure 4. Validation of tumor-associated *ETV1* target genes in cell line models. (A) Using shRNAs directed to *ETV1*, a significant down-regulation of *ETV1* expression was achieved in LNCaP cells, as evaluated both by qRT-PCR and by Western blot analyses. (B) *FKBP10* and *GLYATL2*, two tumor-associated *ETV1* candidate target genes, were shown to be significantly decreased after *ETV1* silencing. (C) *De novo* expression of *ETV1* was stably induced in the benign PNT2 prostate cells, as shown by qRT-PCR and Western blot analyses. (D) *De novo* expression of *ETV1* induced significant up-regulation of *FKBP10* expression in the PNT2-*ETV1*-B cells, which show higher expression of *ETV1*. (E) Box plot distribution of the expression of *FKBP10* among the different sample groups shows a significant up-regulation of *FKBP10* in *ETV1*-positive PCa comparing with other PCa and with NPT samples. $^{**}P < .01$. NS indicates not significant ($P > .05$).

Cell Line Treatment with Epigenetic Modulating Drugs

To evaluate whether *TDRD1* promoter demethylation was regulated by *ERG*, we treated PNT2 cells with *de novo* expression of Δ*ERG* and *ETV1* with 1 μM of the DNA methyltransferases inhibitor 5-aza-2′ deoxycytidine (DAC; Sigma-Aldrich) and with 0.5 μM of the histone deacetylase inhibitor Trichostatin A (TSA; Sigma-Aldrich), both individually and in combination, as described by Costa et al. [23]. After 72 and 24 hours of treatment with DAC and TSA, respectively, DNA and RNA were extracted using the TriplePrep Kit (GE Healthcare), according to the manufacturer's recommendations.

Statistical Analysis

To compare gene expression data between the different sample groups, the Mann-Whitney nonparametric test was applied on RMA-normalized data using the Statistical Package for Social Sciences, version 15.0 (SPSS, Inc, Chicago, IL). Data from qMSP and mRNA expression of *TDRD1* were compared with the Spearman nonparametric correlation test. Student's *t* test was applied to evaluate differences in the expression data obtained by quantitative real-time PCR (qRT-PCR). $P < .05$ was considered statistically significant.

Results

Differential Expression Analysis in Primary Tumors

Expression array data allowed the identification of both specific and shared *ERG* and *ETV1* expression-associated genes (Figure 1). Distribution of samples according to the expression profile of the 22,000 genes shows that the PCa samples form a unique cluster that deviates from the expression profile found in the NPT control samples (Figure 2*A*). Combined analysis of genes differentially expressed among the different sample groups (NPT, ETS-negative PCa, *ERG*-positive PCa and *ETV1*-positive PCa) led to the identification of 57 genes specifically associated with PCa with *ERG* rearrangement (Table W2) and 15 genes specifically associated with PCa with *ETV1* rearrangement (Table W3), with 27 genes being differentially expressed in both PCa subgroups comparing to PCa without ETS rearrangements and with NPT (Table W4). PCA using the expression data of the 99 genes thus selected shows four completely independent sample clusters: NPT controls, ETS-negative PCa, ERG-positive PCa, and ETV1-positive PCa (Figure 2*B*). Hierarchical clustering of the samples according to expression of the 99 genes and of *ERG* and *ETV1* shows clear stratification according to the ETS rearrangement status (Figure 2*C*). Interestingly, the two PCa with other ETS rearrangements (involving *ETV4* and *ETV5*) cluster in close proximity with *ETV1*-positive PCa samples.

Selection of Target Genes for Validation in VCaP and LNCaP Cell Line Models

Using the expression profile of VCaP, LNCaP, PC3, and DU145 cell lines available from Taylor et al. [30] (GSE21034), of our list of 57 *ERG* candidate target genes, only 7 (*ATP8A2*, *CACNA1D*, *HLA-DMB*, *PDE3B*, *PLA1A*, *SH3RF1*, and *TDRD1*) were significantly upregulated and 1 (*TMBIM1*) was significantly downregulated in VCaP cells compared with the other cell lines (Figure W1). Following the same approach, only 2 (*FKBP10* and *GLYATL2*) of the 15 candidate *ETV1* target genes were significantly upregulated in LNCaP cells comparing with the other cell lines, and only 7 (*CDC2L6*, *GRPR*, *KCNH8*, *NCALD*, *PLA2G7*, *TMEM45B*, and *ZNF385B*) of the 27 target genes shared by *ERG* and *ETV1* rearrangements were overexpressed at least in one of the two ETS-positive cell lines comparing with PC3 and DU145 (Figure W1). *In silico* analysis of the ChIP-Seq data set available from Yu et al. [26] confirmed ERG binding to the promoter of both the eight specific and the seven shared ERG candidate target genes in VCaP cells (Table W5).

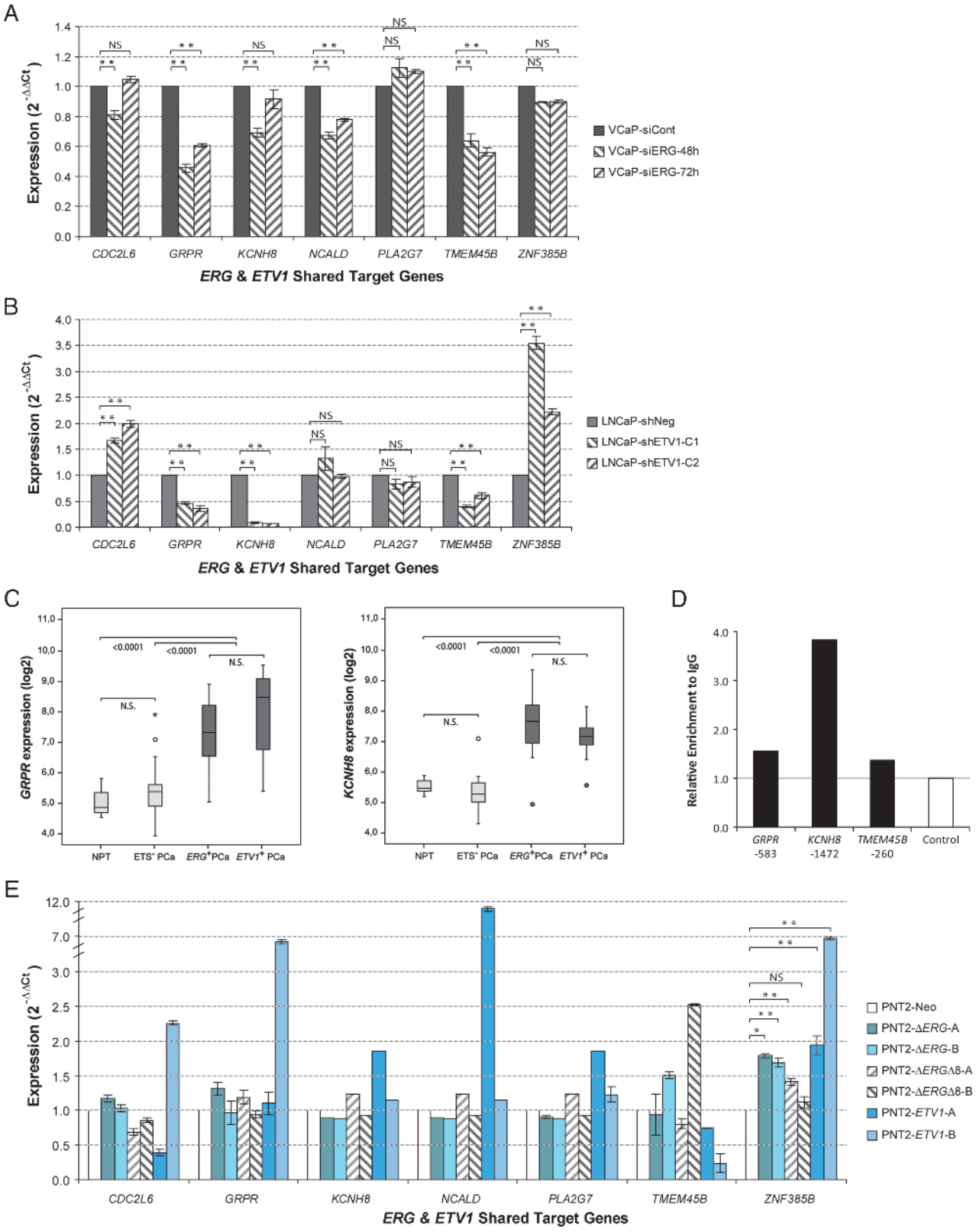

Figure 5. Validation of shared *ERG* and *ETV1* tumor-associated target genes in cell line models. (A and B) Quantitative expression analysis of the seven ETS shared candidate target genes in *ERG*-downregulated VCaP cells and *ETV1*-downregulated LNCaP cells, respectively, shows that *GRPR*, *KCNH8*, and *TMEM45B* are significantly downregulated after silencing of either *ERG* or *ETV1*. (C) Box plot distribution of the expression of *GRPR* (left panel) and *KCNH8* (right panel) among the different prostate sample groups shows significant up-regulation of both genes in *ERG*- and *ETV1*-positive PCa comparing with ETS-negative PCa and with NPT samples. (D) qPCR of ERG-immunoprecipitated chromatin from VCaP cells shows that ERG binds to the *GRPR*, *KCNH8*, and *TMEM45B* promoters. Only the promoter regions that gave a relative enrichment value above the negative control are shown. (E) *De novo* expression of two Δ*ERG* isoforms and of *ETV1* was not sufficient to induce expression of these genes in PNT2 cells. *$P < .05$. **$P < .01$. NS indicates not significant ($P > .05$).

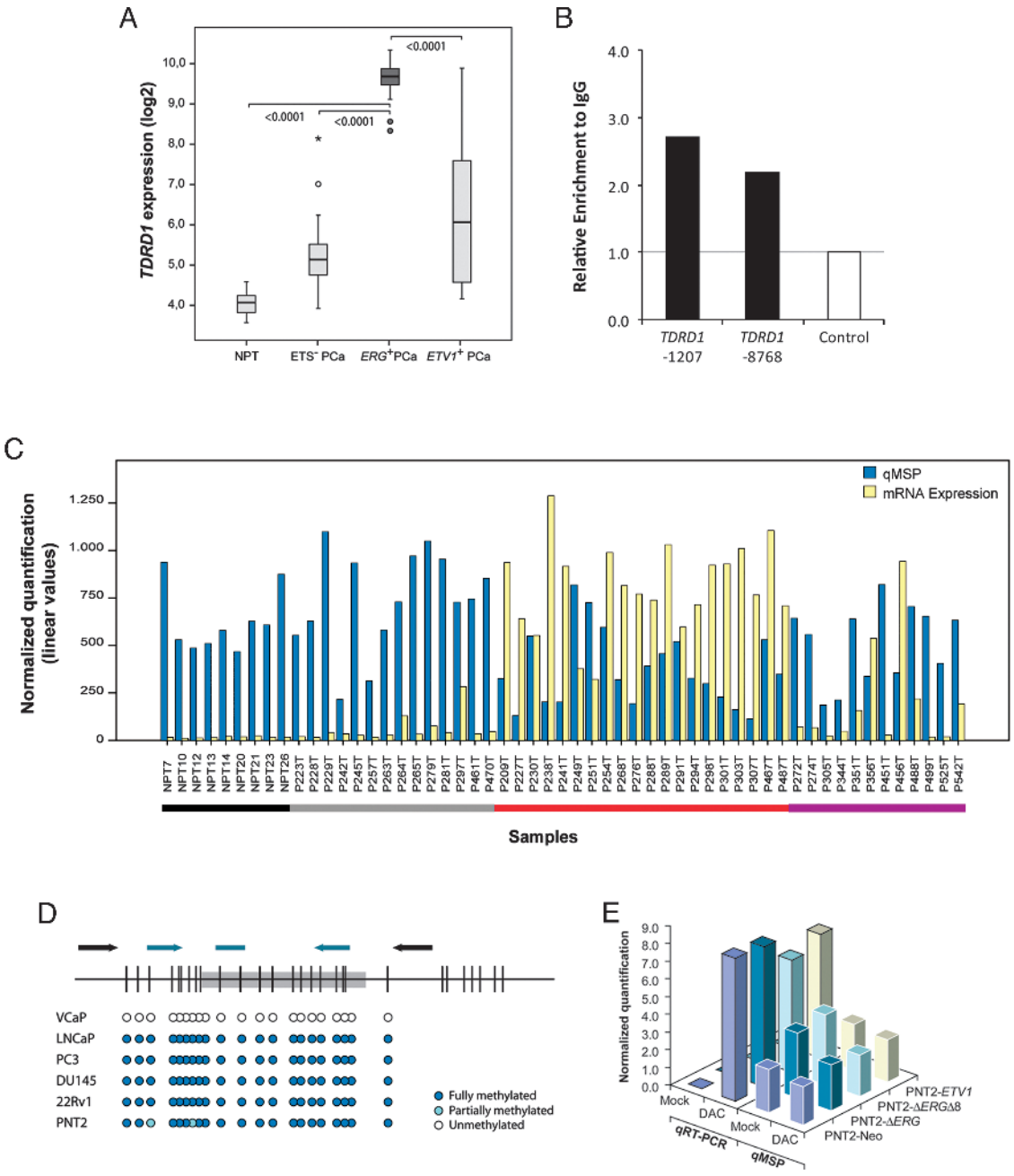

Figure 6. Analysis of the topmost tumor-associated *ERG* target gene – *TDRD1*. (A) Box plot distribution of the nine prostate controls (NPT) and the 48 PCa according to the expression of *TDRD1* shows a significant *P* value comparing *ERG*-positive PCa with other PCa and with NPT. (B) qPCR of ERG-immunoprecipitated chromatin from VCaP cells shows that ERG binds to two regions of the *TDRD1* promoter. Only the promoter regions that gave a relative enrichment value above the negative control are shown. (C) Quantitative expression and methylation levels of *TDRD1* in prostate controls and tumors show an inverse correlation ($r_s = -0.417$, $P = .0015$). NPTs are underlined in black, *ETS*-negative PCa in gray, *ERG*-positive PCa in red, and *ETV1*-positive PCa in purple. (D) Schematic representation of the CpG island found in the *TDRD1* promoter and of the methylation status of each CG dinucleotide in prostate cell lines. The location of the primers used for bisulfite sequencing is shown by black arrows and the location of the primers and the TaqMan probe used for qMSP is shown in blue. (E) Quantitative expression and methylation levels of *TDRD1* in PNT2 cells show that *de novo* expression of two Δ*ERG* isoforms and of *ETV1* does not increase the demethylation-induced expression of *TDRD1* in the presence of DAC.

ERG-*Dependent Deregulation of Tumor-Associated* ERG *Target Genes in VCaP Cells*

Quantitative expression analysis of the eight *ERG* candidate target genes after siRNA-mediated *ERG* silencing in VCaP cells shows that expression of all genes but *SH3RF1* is significantly affected by *ERG* knockdown (Figure 3, *A* and *B*). *De novo* overexpression of the most common *ERG* truncated isoforms (Δ*ERG* and Δ*ERG*Δ8) in the benign prostate cell line PNT2, however, did not show the reverse effect (Figure 3, *C* and *D*). Expression levels of the seven deregulated *ERG* candidate target genes were not affected by *ETV1* silencing in LNCaP cells (data not shown), thus confirming that the observed *ERG*-dependent regulation is specific of tumor cells harboring *ERG* overexpression.

ETV1 *Overexpression Drives Up-regulation of the Tumor-Associated Target* FKBP10

A significant down-regulation of *FKBP10* and *GLYATL2* was observed in the LNCaP-shETV1 clones (Figure 4, *A* and *B*). Interestingly, *de novo* expression of full-length *ETV1* in PNT2 cells showed significant up-regulation of *FKBP10* in the PNT2-*ETV1*-B population (Figure 4C and 4D). These observations were not found in VCaP-siERG cells neither in any of the PNT2-*ERG* cells (data not shown), thus suggesting that *ETV1* overexpression specifically drives *FKBP10* up-regulation in prostate cells.

Shared Tumor-Associated ETS Target Genes Are Regulated by Both ERG *and* ETV1 *in Prostate Cancer Cell Lines*

Quantification of the expression levels of the seven candidate target genes shared by *ERG* and *ETV1* rearrangements showed that *GRPR*, *KCNH8*, and *TMEM45B* are significantly downregulated after silencing of both ETS transcription factors (Figure 5, *A* and *B*). Interestingly, *GRPR* and *KCNH8* were the topmost overexpressed genes of our list of *ERG* and *ETV1* shared candidate target genes (Figure 5*C*). qPCR on the ERG-immunoprecipitated chromatin from VCaP cells showed direct binding of ERG to the promoters of *GRPR* (region −583), *KCNH8* (region −1472), and *TMEM45B* (region −260) (Figure 5*D*).

TDRD1 *Expression Is Regulated by* ERG *in Prostate Tumors Harboring* ERG *Rearrangement*

Considering the highly significant association of our topmost overexpressed gene, *TDRD1*, with PCa harboring *ERG* rearrangements (Figure 6*A*), we first questioned whether *TDRD1* was a direct target of ERG. qPCR on the ERG-immunoprecipitated chromatin from VCaP cells showed that ERG binds to the *TDRD1* promoter in two promoter regions (Figure 6*B*).

Because *TDRD1* is described as a cancer germ line gene regulated by methylation [31], we questioned whether methylation levels of *TDRD1* promoter differ among NPT control samples and the different subgroups of PCa of our series. A CpG island with 28 CpG dinucleotides was found starting at −66 bp of the transcription start site (Ensembl gene ID ENSG00000095627) and covering 330 bp (Figure 6, *C* and *D*). As expected, a significant inverse correlation was obtained between *TDRD1* mRNA expression (exon array data, linear values) and *TDRD1* methylation levels (r_s = −0.417, P = .0015). A significant decrease in *TDRD1* methylation was found between tumors harboring ERG rearrangements and both NPT (P = .004) and tumors without ETS rearrangements (P = .0001), whereas methylation levels of NPT and ETS-negative PCa were not statistically different (P = .124).

Bisulfite sequencing of the *TDRD1* promoter in VCaP, LNCaP, PC3, DU145, 22Rv1, and PNT2 cells showed that the *TDRD1* promoter is completely methylated in all cell lines except in VCaP cells (Figure 6*D*), the only cell line that shows expression of *TDRD1* by qRT-PCR (data not shown). Interestingly, the CpG island completely overlaps with the promoter region at −8768 bp shown to be bound by ERG using ChIP. To evaluate whether *ERG* overexpression modulates the levels of methylation-controlled *TDRD1* expression in prostate cancer cells, we treated PNT2 cell populations (PNT2-*Neo*, PNT2-*ERG*, and PNT2-*ETV1*) with epigenetic modulating drugs. Treatment with DAC induced *TDRD1* expression in all PNT2 cells, and this reexpression was associated with decreased methylation levels of the *TDRD1* promoter (Figure 6*E*). These effects were not observed when cells were treated with TSA alone, and neither were they increased with the combination of TSA and DAC (data not shown).

Discussion

We have analyzed a clinical series of PCa enriched for *ERG* and *ETV1* rearrangements with a genome-scale and exon-level expression microarray platform that ensures robust gene-level expression measures. Of 57 *ERG*-associated genes in primary PCa, 8 were also deregulated in VCaP cells with the *TMPRSS2-ERG* fusion. In fact, seven of these genes were shown to be significantly affected by *ERG* knockdown. Six of these genes (*PLA1A*, *CACNA1D*, *ATP8A2*, *HLA-DMB*, *PDE3B*, and *TDRD1*) have been previously described as coexpressed with *ERG* in prostate cancer, but only *PLA1A* and *CACNA1D* are validated as direct *ERG* target genes [12,18,32–35]. The top-ranked tumor-associated *ERG* target gene in our study was *TDRD1*, and we showed not only that *TDRD1* expression is regulated by methylation of a CpG island located at −66 bp of the transcription start site [31] but also that ERG binds to the unmethylated CpG island of the *TDRD1* promoter in VCaP cells. Although *ERG* silencing in VCaP cells resulted in down-regulation of *TDRD1*, our data on *de novo* overexpression of *ERG* in PNT2 cells suggest that another regulatory mechanism acting upstream of *ERG* actively leads to demethylation of *TDRD1* promoter or that other cofactors may be required for *ERG*-mediated *TDRD1* demethylation. *TDRD1* encodes the tudor domain-containing protein 1 described as involved in male germ cell differentiation and in the small RNAs pathway [36–38]. Although the biologic consequence of overexpressed or reexpressed *TDRD1* is not known, loss of *TDRD1* in germ line cells is associated with changes in small RNA profile and with loss of methylation of L1 transposons [39] and may thus establish a link between *ERG* overexpression and the epigenetic reprogramming described by others [26,40,41].

Of the 15 genes highly associated with tumors harboring *ETV1* rearrangements, only 2 genes were shown to have the expected overexpression in the LNCaP cell line harboring an *ETV1* rearrangement. Both *FKBP10* and *GLYATL2* were significantly downregulated after *ETV1* knockdown, but only *FKBP10* seemed to be upregulated in PNT2 cells with *de novo* expression of *ETV1*. *FKBP10* (FK506-binding protein 10) encodes a member of the highly conserved family of intracellular receptors called immunophilins, which acts as a molecular chaperone in the endoplasmic reticulum [42]. We found no reports on *FKBP10* involvement in prostate carcinogenesis, but other immunophilins, namely *FKBP51* and *FKBP52*, have been described to be androgen regulated and their interaction with androgen receptor (AR) seems to be necessary for AR-mediated proliferation of LNCaP cells [43]. In the same cells, the presence of its ligand, FK506, was sufficient to block several stages of the AR signaling [44]. Taken together, these observations suggest that inhibition of *FKBP10* by FK506 may be a good therapy approach for the treatment of PCa harboring *ETV1* rearrangements. Interestingly, when the expression profiles of the two PCa with *ETV4* and *ETV5* rearrangements were included in the hierarchical clustering, they clustered among the *ETV1*-positive PCa samples. This suggests that the *ETV4* and *ETV5* tumor-associated target genes might be, at least in part, shared with *ETV1*, which, altogether, represent the PEA3 subfamily of ETS transcription factors [45].

Although the identification of specific target genes of *ERG* and *ETV1* rearrangements in PCa is a major finding in this work, the

existence of shared target genes was expected because both genes belong to the same family of transcription factors [46]. In fact, we report a list of 27 target genes shared by *ERG* and *ETV1* rearrangements. *KCNH8* and *NCALD* have been previously associated with tumors harboring *ERG* rearrangements [32–34], but no biologic validation of their *ERG* dependence had been shown. Our results, using the VCaP and LNCaP knockdown cell line models, clearly validate *KCNH8*, *GRPR*, and *TMEM45B* as downstream targets of both *ERG* and *ETV1*, as also indicated by our demonstration of direct binding of ERG to the promoter of these genes using ERG-immunoprecipitated chromatin from VCaP cells. *TMEM45B* encodes a putative membrane protein with unknown function, so its role in prostate carcinogenesis might be worth exploring. Nevertheless, *GRPR*, which encodes the gastrin-releasing peptide receptor, has been described as overexpressed in several cancer types, including PCa [47–51]. Overexpression of *GRPR* was found in androgen-dependent prostate cancer xenografts [52], and it seems to be dependent on AR activation [53]. Recently, Beer et al. [50] described that combined overexpression of *GRPR* and *AR* was associated with a favorable prognosis in patients with PCa. These observations, together with our findings showing *GRPR* overexpression in a high proportion of PCa harboring either *ERG* or *ETV1* rearrangements, warrant further investigation on the cooperation of ETS transcription factors and AR signaling in regulating the expression of *GRPR* in PCa.

Only a fraction of the *ERG* and *ETV1* tumor-associated genes showed the expected expression pattern in VCaP and LNCaP cell lines, the best available *in vitro* models of *ERG*- and *ETV1*-positive PCa. This by no means indicates that the remaining potential ETS target genes found in primary tumors are not relevant for *in vivo* prostate carcinogenesis; it may be that these cell lines have kept only the part of the *in vivo* tumor-derived gene expression signature that was advantageous for *in vitro* survival or the *in vitro* cell line–associated gene expression signature is being modulated by the environmental factors to which cells are exposed. In fact, our PCa series is derived from organ confined or locally advanced tumors [8] removed by radical prostatectomy before any other therapy, meaning that they were, most probably, androgen responsive. Nevertheless, although VCaP and LNCaP cells are androgen responsive [54,55], the gene expression signature available from Taylor et al. [30] and the *ERG* and *ETV1* silencing experiments that were performed were obtained without androgen stimulation. This suggests that the expression of some tumor-associated *ERG* and *ETV1* target genes might be dependent on androgen receptor activation, whereas others might be androgen independent. The same explanation may be operative with the overall absence of effect on the tested target genes that was observed with *de novo* expression of either Δ*ERG* isoforms or *ETV1* in the benign PNT2 cells, which are also androgen sensitive [56]. Silencing and *de novo* expression of *ERG* and *ETV1* in these cell line models under androgen stimulation, together with cell line–based assays focusing in specific *ERG* and *ETV1* targets, would be useful to clarify the cooperativity/dependence of these ETS transcription factors and/or AR signaling.

In conclusion, differential expression profile of tumors harboring either *ERG* or *ETV1* rearrangements allowed the identification of both specific and shared ETS downstream targets. From detailed studies in prostate cancer models, we have validated ETS-dependent expression of seven *ERG*-specific, two *ETV1*-specific, and three *ERG* and *ETV1* shared target genes. *TDRD1*, *FKBP10*, and *GRPR* are promising therapeutic targets and can serve as diagnostic markers for molecular subtypes of PCa harboring specific fusion gene rearrangements.

References

[1] Tomlins SA, Rhodes DR, Perner S, Dhanasekaran SM, Mehra R, Sun XW, Varambally S, Cao X, Tchinda J, Kuefer R, et al. (2005). Recurrent fusion of *TMPRSS2* and *ETS* transcription factor genes in prostate cancer. *Science* **310**, 644–648.

[2] Clark JP and Cooper CS (2009). *ETS* gene fusions in prostate cancer. *Nat Rev Urol* **6**, 429–439.

[3] Kumar-Sinha C, Tomlins SA, and Chinnaiyan AM (2008). Recurrent gene fusions in prostate cancer. *Nat Rev Cancer* **8**, 497–511.

[4] Han B, Mehra R, Dhanasekaran SM, Yu J, Menon A, Lonigro RJ, Wang X, Gong Y, Wang L, Shankar S, et al. (2008). A fluorescence *in situ* hybridization screen for E26 transformation-specific aberrations: identification of DDX5-ETV4 fusion protein in prostate cancer. *Cancer Res* **68**, 7629–7637.

[5] Helgeson BE, Tomlins SA, Shah N, Laxman B, Cao Q, Prensner JR, Cao X, Singla N, Montie JE, Varambally S, et al. (2008). Characterization of *TMPRSS2:ETV5* and *SLC45A3:ETV5* gene fusions in prostate cancer. *Cancer Res* **68**, 73–80.

[6] Hermans KG, Bressers AA, van der Korput HA, Dits NF, Jenster G, and Trapman J (2008). Two unique novel prostate-specific and androgen-regulated fusion partners of *ETV4* in prostate cancer. *Cancer Res* **68**, 3094–3098.

[7] Tomlins SA, Mehra R, Rhodes DR, Smith LR, Roulston D, Helgeson BE, Cao X, Wei JT, Rubin MA, Shah RB, et al. (2006). *TMPRSS2:ETV4* gene fusions define a third molecular subtype of prostate cancer. *Cancer Res* **66**, 3396–3400.

[8] Paulo P, Barros-Silva JD, Ribeiro FR, Ramalho-Carvalho J, Jeronimo C, Henrique R, Lind GE, Skotheim RI, Lothe RA, and Teixeira MR (2012). FLI1 is a novel ETS transcription factor involved in gene fusions in prostate cancer. *Genes Chromosomes Cancer* **51**, 240–249.

[9] Uren A and Toretsky JA (2005). Ewing's sarcoma oncoprotein EWS-FLI1: the perfect target without a therapeutic agent. *Future Oncol* **1**, 521–528.

[10] Gupta S, Iljin K, Sara H, Mpindi JP, Mirtti T, Vainio P, Rantala J, Alanen K, Nees M, and Kallioniemi O (2010). FZD4 as a mediator of *ERG* oncogene–induced WNT signaling and epithelial-to-mesenchymal transition in human prostate cancer cells. *Cancer Res* **70**, 6735–6745.

[11] Mohamed AA, Tan SH, Sun C, Shaheduzzaman S, Hu Y, Petrovics G, Chen Y, Sesterhenn IA, Li H, Sreenath T, et al. (2011). *ERG* oncogene modulates prostaglandin signaling in prostate cancer cells. *Cancer Biol Ther* **11**, 410–417.

[12] Tomlins SA, Laxman B, Varambally S, Cao X, Yu J, Helgeson BE, Cao Q, Prensner JR, Rubin MA, Shah RB, et al. (2008). Role of the *TMPRSS2-ERG* gene fusion in prostate cancer. *Neoplasia* **10**, 177–188.

[13] Hermans KG, van der Korput HA, van Marion R, van de Wijngaart DJ, Ziel-van der Made A, Dits NF, Boormans JL, van der Kwast TH, van Dekken H, Bangma CH, et al. (2008). Truncated *ETV1*, fused to novel tissue-specific genes, and full-length *ETV1* in prostate cancer. *Cancer Res* **68**, 7541–7549.

[14] Tomlins SA, Laxman B, Dhanasekaran SM, Helgeson BE, Cao X, Morris DS, Menon A, Jing X, Cao Q, Han B, et al. (2007). Distinct classes of chromosomal rearrangements create oncogenic *ETS* gene fusions in prostate cancer. *Nature* **448**, 595–599.

[15] Cai C, Hsieh CL, Omwancha J, Zheng Z, Chen SY, Baert JL, and Shemshedini L (2007). *ETV1* is a novel androgen receptor–regulated gene that mediates prostate cancer cell invasion. *Mol Endocrinol* **21**, 1835–1846.

[16] Wang J, Cai Y, Ren C, and Ittmann M (2006). Expression of variant *TMPRSS2/ERG* fusion messenger RNAs is associated with aggressive prostate cancer. *Cancer Res* **66**, 8347–8351.

[17] Owczarek CM, Portbury KJ, Hardy MP, O'Leary DA, Kudoh J, Shibuya K, Shimizu N, Kola I, and Hertzog PJ (2004). Detailed mapping of the *ERG-ETS2* interval of human chromosome 21 and comparison with the region of conserved synteny on mouse chromosome 16. *Gene* **324**, 65–77.

[18] Wang J, Cai Y, Yu W, Ren C, Spencer DM, and Ittmann M (2008). Pleiotropic biological activities of alternatively spliced *TMPRSS2/ERG* fusion gene transcripts. *Cancer Res* **68**, 8516–8524.

[19] Schmittgen TD and Livak KJ (2008). Analyzing real-time PCR data by the comparative *C*(T) method. *Nat Protoc* **3**, 1101–1108.

[20] Pearson H and Stirling D (2003). DNA extraction from tissue. *Methods Mol Biol* **226**, 33–34.

[21] Eads CA, Danenberg KD, Kawakami K, Saltz LB, Blake C, Shibata D, Danenberg PV, and Laird PW (2000). MethyLight: a high-throughput assay to measure DNA methylation. *Nucleic Acids Res* **28**, E32.

[22] Costa VL, Henrique R, Ribeiro FR, Carvalho JR, Oliveira J, Lobo F, Teixeira MR, and Jeronimo C (2010). Epigenetic regulation of Wnt signaling pathway in urological cancer. *Epigenetics* **5**, 343–351.

[23] Costa VL, Henrique R, Danielsen SA, Duarte-Pereira S, Eknaes M, Skotheim RI, Rodrigues A, Magalhaes JS, Oliveira J, Lothe RA, et al. (2010). Three epigenetic biomarkers, *GDF15*, *TMEFF2*, and *VIM*, accurately predict bladder cancer from DNA-based analyses of urine samples. *Clin Cancer Res* **16**, 5842–5851.

[24] Barros R, da Costa LT, Pinto-de-Sousa J, Duluc I, Freund JN, David L, and Almeida R (2011). CDX2 autoregulation in human intestinal metaplasia of the stomach: impact on the stability of the phenotype. *Gut* **60**, 290–298.

[25] Ribeiro FR, Paulo P, Costa VL, Barros-Silva JD, Ramalho-Carvalho J, Jeronimo C, Henrique R, Lind GE, Skotheim RI, Lothe RA, et al. (2011). Cysteine-rich secretory protein-3 (CRISP3) is strongly up-regulated in prostate carcinomas with the *TMPRSS2-ERG* fusion gene. *PLoS One* **6**, e22317.

[26] Yu J, Mani RS, Cao Q, Brenner CJ, Cao X, Wang X, Wu L, Li J, Hu M, Gong Y, et al. (2010). An integrated network of androgen receptor, polycomb, and *TMPRSS2-ERG* gene fusions in prostate cancer progression. *Cancer Cell* **17**, 443–454.

[27] Sandelin A, Wasserman WW, and Lenhard B (2004). ConSite: Web-based prediction of regulatory elements using cross-species comparison. *Nucleic Acids Res* **32**, W249–W252.

[28] Wei GH, Badis G, Berger MF, Kivioja T, Palin K, Enge M, Bonke M, Jolma A, Varjosalo M, Gehrke AR, et al. (2010). Genome-wide analysis of ETS-family DNA-binding *in vitro* and *in vivo*. *EMBO J* **29**, 2147–2160.

[29] Massie CE and Mills IG (2011). Global identification of androgen response elements. *Methods Mol Biol* **776**, 255–273.

[30] Taylor BS, Schultz N, Hieronymus H, Gopalan A, Xiao Y, Carver BS, Arora VK, Kaushik P, Cerami E, Reva B, et al. (2010). Integrative genomic profiling of human prostate cancer. *Cancer Cell* **18**, 11–22.

[31] Loriot A, Boon T, and De Smet C (2003). Five new human cancer—germline genes identified among 12 genes expressed in spermatogonia. *Int J Cancer* **105**, 371–376.

[32] Glinsky GV, Glinskii AB, Stephenson AJ, Hoffman RM, and Gerald WL (2004). Gene expression profiling predicts clinical outcome of prostate cancer. *J Clin Invest* **113**, 913–923.

[33] Jhavar S, Brewer D, Edwards S, Kote-Jarai Z, Attard G, Clark J, Flohr P, Christmas T, Thompson A, Parker M, et al. (2009). Integration of *ERG* gene mapping and gene-expression profiling identifies distinct categories of human prostate cancer. *BJU Int* **103**, 1256–1269.

[34] Jhavar S, Reid A, Clark J, Kote-Jarai Z, Christmas T, Thompson A, Woodhouse C, Ogden C, Fisher C, Corbishley C, et al. (2008). Detection of *TMPRSS2-ERG* translocations in human prostate cancer by expression profiling using GeneChip Human Exon 1.0 ST arrays. *J Mol Diagn* **10**, 50–57.

[35] Washington MN and Weigel NL (2010). 1{alpha},25-Dihydroxyvitamin D_3 inhibits growth of VCaP prostate cancer cells despite inducing the growth-promoting *TMPRSS2:ERG* gene fusion. *Endocrinology* **151**, 1409–1417.

[36] Chuma S, Hosokawa M, Kitamura K, Kasai S, Fujioka M, Hiyoshi M, Takamune K, Noce T, and Nakatsuji N (2006). *Tdrd1/Mtr-1*, a tudor-related gene, is essential for male germ-cell differentiation and nuage/germinal granule formation in mice. *Proc Natl Acad Sci USA* **103**, 15894–15899.

[37] Kojima K, Kuramochi-Miyagawa S, Chuma S, Tanaka T, Nakatsuji N, Kimura T, and Nakano T (2009). Associations between PIWI proteins and TDRD1/MTR-1 are critical for integrated subcellular localization in murine male germ cells. *Genes Cells* **14**, 1155–1165.

[38] Wang J, Saxe JP, Tanaka T, Chuma S, and Lin H (2009). Mili interacts with tudor domain-containing protein 1 in regulating spermatogenesis. *Curr Biol* **19**, 640–644.

[39] Reuter M, Chuma S, Tanaka T, Franz T, Stark A, and Pillai RS (2009). Loss of the Mili-interacting tudor domain-containing protein-1 activates transposons and alters the Mili-associated small RNA profile. *Nat Struct Mol Biol* **16**, 639–646.

[40] Bjorkman M, Iljin K, Halonen P, Sara H, Kaivanto E, Nees M, and Kallioniemi OP (2008). Defining the molecular action of HDAC inhibitors and synergism with androgen deprivation in ERG-positive prostate cancer. *Int J Cancer* **123**, 2774–2781.

[41] Iljin K, Wolf M, Edgren H, Gupta S, Kilpinen S, Skotheim RI, Peltola M, Smit F, Verhaegh G, Schalken J, et al. (2006). *TMPRSS2* fusions with oncogenic *ETS* factors in prostate cancer involve unbalanced genomic rearrangements and are associated with HDAC1 and epigenetic reprogramming. *Cancer Res* **66**, 10242–10246.

[42] Patterson CE, Schaub T, Coleman EJ, and Davis EC (2000). Developmental regulation of FKBP65. An ER-localized extracellular matrix binding-protein. *Mol Biol Cell* **11**, 3925–3935.

[43] Febbo PG, Lowenberg M, Thorner AR, Brown M, Loda M, and Golub TR (2005). Androgen mediated regulation and functional implications of fkbp51 expression in prostate cancer. *J Urol* **173**, 1772–1777.

[44] Periyasamy S, Warrier M, Tillekeratne MP, Shou W, and Sanchez ER (2007). The immunophilin ligands cyclosporin A and FK506 suppress prostate cancer cell growth by androgen receptor–dependent and –independent mechanisms. *Endocrinology* **148**, 4716–4726.

[45] de Launoit Y, Baert JL, Chotteau-Lelievre A, Monte D, Coutte L, Mauen S, Firlej V, Degerny C, and Verreman K (2006). The Ets transcription factors of the PEA3 group: transcriptional regulators in metastasis. *Biochim Biophys Acta* **1766**, 79–87.

[46] Hollenhorst PC, Shah AA, Hopkins C, and Graves BJ (2007). Genome-wide analyses reveal properties of redundant and specific promoter occupancy within the *ETS* gene family. *Genes Dev* **21**, 1882–1894.

[47] Chao C, Ives K, Hellmich HL, Townsend CM Jr, and Hellmich MR (2009). Gastrin-releasing peptide receptor in breast cancer mediates cellular migration and interleukin-8 expression. *J Surg Res* **156**, 26–31.

[48] Fleischmann A, Waser B, and Reubi JC (2009). High expression of gastrin-releasing peptide receptors in the vascular bed of urinary tract cancers: promising candidates for vascular targeting applications. *Endocr Relat Cancer* **16**, 623–633.

[49] Qiao J, Kang J, Ishola TA, Rychahou PG, Evers BM, and Chung DH (2008). Gastrin-releasing peptide receptor silencing suppresses the tumorigenesis and metastatic potential of neuroblastoma. *Proc Natl Acad Sci USA* **105**, 12891–12896.

[50] Beer M, Montani M, Gerhardt J, Wild PJ, Hany TF, Hermanns T, Muntener M, and Kristiansen G (2012). Profiling gastrin-releasing peptide receptor in prostate tissues: clinical implications and molecular correlates. *Prostate* **72**, 318–325.

[51] Thomas SM, Grandis JR, Wentzel AL, Gooding WE, Lui VW, and Siegfried JM (2005). Gastrin-releasing peptide receptor mediates activation of the epidermal growth factor receptor in lung cancer cells. *Neoplasia* **7**, 426–431.

[52] de Visser M, van Weerden WM, de Ridder CM, Reneman S, Melis M, Krenning EP, and de Jong M (2007). Androgen-dependent expression of the gastrin-releasing peptide receptor in human prostate tumor xenografts. *J Nucl Med* **48**, 88–93.

[53] Schroeder RP, de Visser M, van Weerden WM, de Ridder CM, Reneman S, Melis M, Breeman WA, Krenning EP, and de Jong M (2010). Androgen-regulated gastrin-releasing peptide receptor expression in androgen-dependent human prostate tumor xenografts. *Int J Cancer* **126**, 2826–2834.

[54] Loberg RD, St John LN, Day LL, Neeley CK, and Pienta KJ (2006). Development of the VCaP androgen-independent model of prostate cancer. *Urol Oncol* **24**, 161–168.

[55] Olea N, Sakabe K, Soto AM, and Sonnenschein C (1990). The proliferative effect of "anti-androgens" on the androgen-sensitive human prostate tumor cell line LNCaP. *Endocrinology* **126**, 1457–1463.

[56] Blanchere M, Berthaut I, Portois MC, Mestayer C, and Mowszowicz I (1998). Hormonal regulation of the androgen receptor expression in human prostatic cells in culture. *J Steroid Biochem Mol Biol* **66**, 319–326.

Table W1. Assay ID or Sequence of the Primers and Probes Used in This Study.

Assay	Assay/Primer Name	Assay ID/Primer Sequence 5′-3′
CDS-PCR	ΔERG-F	*CTAGGCGCCGGAATTCTAGGCGCGAGCTAAGCAGGAG
CDS-PCR	ΔERG-R	*CGGTAGAATTAGATCTTCCGATAGAGTTTGTGGCGATG
CDS-PCR	ETV1-F	*CTAGGCGCCGGAATTCAGCTGAGATTTGCGAAGAGC
CDS-PCR	ETV1-R	*CGGTAGAATTAGATCTGCCCTGCTTGACTGTCACTT
qRT-PCR	ATP8A2	Hs00185259_m1
qRT-PCR	CACNA1D	Hs00167753_m1
qRT-PCR	CDK19	Hs00292369_m1
qRT-PCR	ERG	Hs01554635_m1
qRT-PCR	ETV1	Hs00951941_m1
qRT-PCR	FKBP10	Hs00222557_m1
qRT-PCR	GHR	Hs01075601_m1
qRT-PCR	GLYATL2	Hs00332757_m1
qRT-PCR	GRPR	Hs01055872_m1
qRT-PCR	HLA-DMB	Hs00157943_m1
qRT-PCR	KCNH8	Hs00292491_m1
qRT-PCR	NCALD	Hs00230737_m1
qRT-PCR	PDE3B	Hs00265322_m1
qRT-PCR	PLA1A	Hs01056915_m1
qRT-PCR	PLA2G7	Hs00173726_m1
qRT-PCR	SH3RF1	Hs00325806_m1
qRT-PCR	TDRD1	Hs00229805_m1
qRT-PCR	TMBIM1	Hs00223351_m1
qRT-PCR	TMEM45B	Hs00431155_m1
qRT-PCR	ZNF385B	Hs00332216_m1
qRT-PCR	GUSB	4333767F
qMSP	TDRD1-F	ATATTGAGTTGTACGTGGACGC
qMSP	TDRD1-R	GAATCCGAACCTATCTCTACGA
qMSP	TDRD1-P	CCTCGCCTCCAATCCCCAATACG
qMSP	ACTB-F	TGGTGATGGAGGAGGTTTAGTAAGT
qMSP	ACTB-R	AACCAATAAAACCTACTCCTCCCTTAA
qMSP	ACTB-P	ACCACCACCCAACACACAATAACAAACACA
BSP	TDRD1-F	TTGTAAAGGAATTTTTTGAGTTTG
BSP	TDRD1-R	CCTTCATACAAACCCTCTCC
ChIP-qPCR	pTDRD1-1207F	TCAGCCTGTCCCTTCAATTTAG
ChIP-qPCR	pTDRD1-1207R	CCCTCGAAAGTAGGGAACTCTT
ChIP-qPCR	pTDRD1-3196F	TGCTACAGTTTCTGGAGGTTCT
ChIP-qPCR	pTDRD1-3196R	TGCAATAGCCACAGGTGAAG
ChIP-qPCR	pTDRD1-7686F	GGTTCCACAGGAATGGAAGA
ChIP-qPCR	pTDRD1-7686R	TGTAAAATGCAGAGGGCAGTAG
ChIP-qPCR	pTDRD1-8768F	CCAAGTGACCTTCGAGGAGA
ChIP-qPCR	pTDRD1-8768R	GTCCACGTGCAACTCAATGT
ChIP-qPCR	pKCNH8-797F	GGATGGGCCTCACAACTAAC
ChIP-qPCR	pKCNH8-797R	TTGGAGAAAGGGAGGAGACA
ChIP-qPCR	pKCNH8-1472F	CCGAGTTCCTGGAGATCAGA
ChIP-qPCR	pKCNH8-1472R	ACCCAGAGCCCGAACTTTAT
ChIP-qPCR	pKCNH8-3506F	TGTGCTTGCTTTCAATCTGG
ChIP-qPCR	pKCNH8-3506R	CTTGGGGCTTCAGTTATTGG
ChIP-qPCR	pGRPR-583F	TGGGCAGTGATTGAAGTGTC
ChIP-qPCR	pGRPR-583R	GCACTGAGAAATCCTCAAATCC
ChIP-qPCR	pGRPR-1386F	TGGCTAAAGGTCTAAGCCTG
ChIP-qPCR	pGRPR-1386R	CGGCATTTTGATGCAGCTAT
ChIP-qPCR	pGRPR-4858F	TCCTTCCCTCACACCCTGTA
ChIP-qPCR	pGRPR-4858R	ATGCACCCACAGGTAACACC
ChIP-qPCR	pTMEM45B-260F	CCCCACCCTCATCCTTTTAT
ChIP-qPCR	pTMEM45B-260R	CCACGTTAAGAAGGATCAACAC
ChIP-qPCR	pTMEM45B-2847F	ACATGGATGCCACCAAGATT
ChIP-qPCR	pTMEM45B-2847R	GGGTCTCAGAGATCACTGCCTA
ChIP-qPCR	pTMEM45B-5687F	GGTGATGCCTGACAATGATG
ChIP-qPCR	pTMEM45B-5687R	AGCCACTTTCAACCCTTTCA

F indicates forward; P, probe (5′ FAM and 3′TAMRA); R, reverse.
*Underlined nucleotides are the In-fusion link for cloning, not gene specific.

Table W2. Tumor-Associated ERG-Specific Target Genes.

Gene Symbol	Cytoband	mRNA Accession	Description
ACADVL	17p13-p11	NM_000018	Acyl-coenzyme A dehydrogenase, very long chain
ACER3	11q13.5	NM_018367	Alkaline ceramidase 3
ALDH2	12q24.2	NM_000690	Aldehyde dehydrogenase 2 family (mitochondrial)
ALOX15	17p13.3	NM_001140	Arachidonate 15-lipoxygenase
AMPD3	11p15	NM_001025390	Adenosine monophosphate deaminase (isoform E)
ANG	14q11.1-q11.2	NM_001145	Angiogenin, ribonuclease, RNAse A family, 5
ATP8A2	13q12	NM_016529	ATPase, aminophospholipid transporter-like, class I, type 8A, member 2
AUTS2	7q11.22	NM_015570	Autism susceptibility candidate 2
AZGP1	7q22.1	NM_001185	α-2-glycoprotein 1, zinc-binding
BCR	22q11|22q11.23	NM_004327	Breakpoint cluster region
C4orf18	4q32.1	NM_001128424	Chromosome 4 open reading frame 18
CACNA1D	3p14.3	NM_000720	Calcium channel, voltage-dependent, L-type, α 1D subunit
CD44	11p13	NM_000610	CD44 molecule (Indian blood group)
CDH7	18q22-q23	NM_033646	Cadherin 7, type 2
CLUL1	18p11.32	NM_014410	Clusterin-like 1 (retinal)
CRYM	16p13.11-p12.3	NM_001888	Crystallin, mu
CST3	20p11.21	NM_000099	Cystatin C
EFHD2	1p36.21	NM_024329	EF-hand domain family, member D_2
FRK	6q21-q22.3	NM_002031	Fyn-related kinase
GDA	9q21.13	NM_004293	Guanine deaminase
GPRC5D	12p13.3	NM_018654	G protein-coupled receptor, family C, group 5, member D
HDAC1	1p34	NM_004964	Histone deacetylase 1
HLA-DMB	6p21.3	NM_002118	Major histocompatibility complex, class II, DM β
HPS1	10q23.1-q23.3	NM_000195	Hermansky-Pudlak syndrome 1
KAZALD1	10q24.31	NM_030929	Kazal-type serine peptidase inhibitor domain 1
KCNN2	5q22.3	NM_021614	Potassium intermediate/small conductance calcium-activated channel, subfamily N, member 2
KCNS3	2p24	NM_002252	Potassium voltage-gated channel, delayed-rectifier, subfamily S, member 3
KIF16B	20p11.23	NM_024704	Kinesin family member 16B
LIMK2	22q12.2	NM_016733	LIM domain kinase 2
MAPK6	15q21	NM_002748	Mitogen-activated protein kinase 6
MCOLN2	1p22	NM_153259	Mucolipin 2
MCOLN3	1p22.3	NM_018298	Mucolipin 3
MPPED2	11p13	NM_001584	Metallophosphoesterase domain-containing 2
MUM1L1	Xq22.3	NM_152423	Melanoma-associated antigen (mutated) 1-like 1
MYO6	6q13	NM_004999	Myosin VI
OGDHL	10q11.23	NM_018245	Oxoglutarate dehydrogenase-like
PCDHB9	5q31	NM_019119	Protocadherin β 9
PDE3B	11p15.1	NM_000922	Phosphodiesterase 3B, cGMP-inhibited
PDP1	8q22.1	NM_001161778	Pyruvate dehyrogenase phosphatase catalytic subunit 1
PHLDB2	3q13.2	NM_001134438	Pleckstrin homology-like domain, family B, member 2
PLA1A	3q13.13-q13.2	NM_015900	Phospholipase A1 member A
PNKD	2q35	NM_015488	Paroxysmal nonkinesigenic dyskinesia
PRPS2	Xp22.3-p22.2	NM_001039091	Phosphoribosyl pyrophosphate synthetase 2
PRR15	7p14.3	NM_175887	Proline-rich 15
RAB27A	15q15-q21.1	NM_004580	RAB27A, member RAS oncogene family
RAB30	11q12-q14	NM_014488	RAB30, member RAS oncogene family
RICH2	17p12	NM_014859	Rho-type GTPase-activating protein RICH2
SEMA4G	10q24.31	NM_017893	Sema domain, immunoglobulin domain (Ig), transmembrane domain (TM) and short cytoplasmic domain, (semaphorin) 4G
SH3RF1	4q32.3-q33	NM_020870	SH3 domain-containing ring finger 1
SLCO1B3	12p12	NM_019844	Solute carrier organic anion transporter family, member 1B3
SMOC2	6q27	NM_022138	SPARC-related modular calcium binding 2
TDRD1	10q25.3	NM_198795	Tudor domain-containing 1
TMBIM1	2p24.3-p24.1	NM_022152	Transmembrane BAX inhibitor motif containing 1
TMEM134	11q13.2	NM_025124	Transmembrane protein 134
TMEM26	10q21.2	NM_178505	Transmembrane protein 26
VLDLR	9p24	NM_003383	Very low density lipoprotein receptor
ZNF217	20q13.2	NM_006526	Zinc finger protein 217

Table W3. Tumor-Associated *ETV1*-Specific Target Genes.

Gene Symbol	Cytoband	mRNA Accession	Description
ACACA	17q21	NM_198839	Acetyl-coenzyme A carboxylase α
BOK	2q37.3	NM_032515	BCL2-related ovarian killer
COL9A2	1p33-p32	NM_001852	Collagen, type IX, α2
FKBP10	17q21.2	NM_021939	FK506 binding protein 10, 65 kDa
GLYATL2	11q12.1	NM_145016	Glycine-*N*-acyltransferase-like 2
MTNR1A	4q35.1	NM_005958	Melatonin receptor 1A
PROS1	3q11.2	NM_000313	Protein S (α)
SIPA1	11q13	NM_153253	Signal-induced proliferation–associated 1
SLC16A1	1p12	NM_003051	Solute carrier family 16, member 1 (monocarboxylic acid transporter 1)
SLC45A2	5p13.2	NM_016180	Solute carrier family 45, member 2
SLC4A10	2q23-q24	NM_022058	Solute carrier family 4, sodium bicarbonate transporter, member 10
SRGAP1	12q14.2	NM_020762	SLIT-ROBO Rho GTPase activating protein 1
SYT6	1p13.2	NM_205848	Synaptotagmin VI
TWIST1	7p21.2	NM_000474	Twist homolog 1 (*Drosophila*)
VSTM2L	20q11.23	NM_080607	V-set and transmembrane domain-containing 2 like

Table W4. Tumor-Associated *ETS* Shared Target Genes.

Gene Symbol	Cytoband	mRNA Accession	Description
APLN	Xq25-q26.3	NM_017413	Apelin
CDC2L6	6q21	NM_015076	Cell division cycle 2-like 6 (CDK8-like)
CHN2	7p15.3	NM_004067	Chimerin (chimaerin) 2
CLYBL	13q32	NM_206808	Citrate lyase β like
CSGALNACT1	8p21.3	NM_018371	Chondroitin sulfate *N*-acetylgalactosaminyltransferase 1
DLX1	2q32	NM_178120	Distal-less homeobox 1
FAM81A	15q22.2	NM_152450	Family with sequence similarity 81, member A
FANK1	10q26.2	NM_145235	Fibronectin type III and ankyrin repeat domains 1
FOXD1	5q12-q13	NM_004472	Forkhead box D1
GHR	5p13-p12	NM_000163	Growth hormone receptor (GHR), mRNA
GRPR	Xp22.2-p22.13	NM_005314	Gastrin-releasing peptide receptor
KCNC2	12q14.1	NM_139136	Potassium voltage-gated channel, Shaw-related subfamily, member 2
KCNH8	3p24.3	NM_144633	Potassium voltage-gated channel, subfamily H (eag-related), member 8
MYO1E	15q21-q22	NM_004998	Myosin IE
NCALD	8q22.2	NM_001040624	Neurocalcin delta
NKAIN1	1p35.2	NM_024522	Na^+/K^+ transporting ATPase interacting 1
NOSTRIN	2q24.3-q31.1	NM_001039724	Nitric oxide synthase trafficker
PLA2G7	6p21.2-p12	NM_005084	Phospholipase A2, group VII (platelet-activating factor acetylhydrolase, plasma)
PPFIBP2	11p15.4	NM_003621	PTPRF interacting protein, binding protein 2 (liprin β2)
REXO2	11q23.1-q23.2	NM_015523	REX2, RNA exonuclease 2 homolog (*Saccharomyces cerevisiae*)
SDK1	7p22.2	NM_152744	Sidekick homolog 1, cell adhesion molecule (chicken)
SNX24	5q23.2	NM_014035	Sorting nexin 24
TMEM178	2p22.1	NM_152390	Transmembrane protein 178
TMEM45B	11q24.3	NM_138788	Transmembrane protein 45B
ZNF385B	2q31.2-q31.3	NM_152520	Zinc finger protein 385B
ZNF652	17q21.32-q21.33	NM_001145365	Zinc finger protein 652
ZNF765	19q13.42	NM_001040185	Zinc finger protein 765

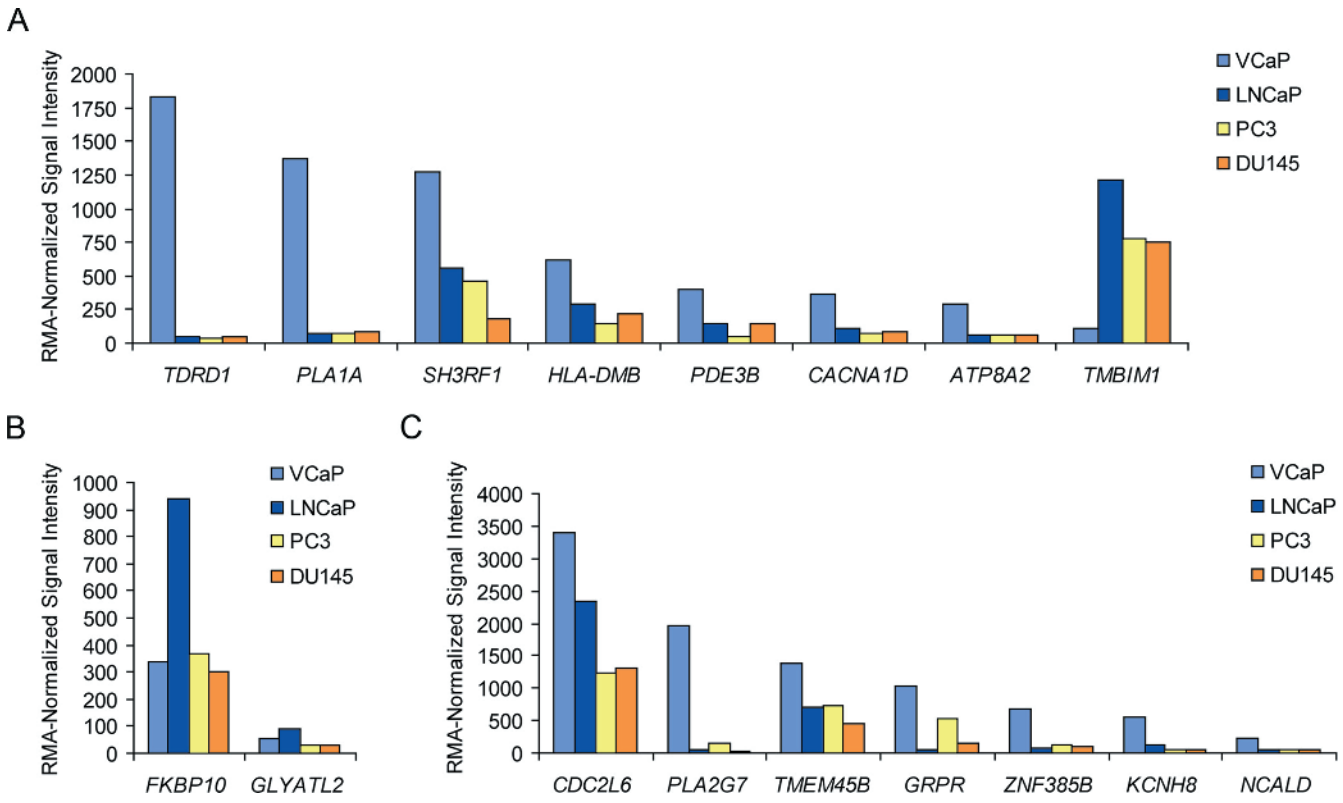

Figure W1. Basal expression levels of the selected ETS target genes in VCaP, LNCaP, PC3, and DU145 cell lines, obtained from the RMA-normalized signal intensity data publicly available from Taylor et al. [30] (GSE21034). (A) Basal expression levels of the eight tumor-associated *ERG*-specific candidate target genes. (B) Basal expression levels of the two tumor-associated *ETV1*-specific candidate target genes. (C) Basal expression levels of the seven tumor-associated *ERG* and *ETV1* shared candidate target genes.

Table W5. *ERG* Binding Sites to the Selected Target Genes [26].

Target	Coordinates (Peak)	Peak Height	Peak Width
ATP8A2	chr13:24,844,894-24,845,182	13.6548	289
	chr13:24,960,106-24,960,310	10.6179	205
	chr13:24,966,222-24,966,790	29.0745	569
	chr13:24,967,021-24,967,552	51.4902	532
	chr13:24,981,947-24,982,277	14.3591	331
	chr13:24,968,575-24,968,953	12.2229	379
	chr13:25,047,778-25,047,926	10.0191	149
	chr13:25,159,694-25,160,317	18.6479	624
	chr13:25,435,965-25,436,267	12.0351	303
	chr13:25,443,584-25,443,980	16.0235	397
	chr13:25,450,401-25,450,626	12.8697	226
	chr13:25,492,200-25,492,681	22.8975	482
CACNA1D	chr3:53,494,975-53,495,558	93.0446	583
	chr3:53,543,934-53,544,673	25.4475	740
	chr3:53,503,125-53,503,899	15.0684	775
	chr3:53,515,374-53,515,828	24.2029	455
	chr3:53,623,475-53,623,677	11.7889	203
CDC2L6	chr6:111,243,178-111,243,861	18.2715	684
	chr6:111,051,167-111,051,366	12.5119	200
	chr6:111,241,751-111,241,952	14.04	202
	chr6:111,117,200-111,117,567	119.945	368
GRPR	chrX:16,051,325-16,051,526	10.369	202
HLA-DMB	chr6:33,017,157-33,017,600	21.7845	444
KCNH8	chr3:19,163,071-19,164,838	62.0921	1768
	chr3:19,233,172-19,233,503	21.5962	332
	chr3:19,272,826-19,273,052	11.42	227
NCALD	chr8:103,206,257-103,206,743	37.8902	487
	chr8:103,204,576-103,205,659	11.8456	1084
	chr8:103,190,344-103,190,556	11.8066	213
	chr8:103,189,323-103,190,009	23.2166	687
	chr8:103,186,224-103,186,529	12.561	306
	chr8:103,112,338-103,112,871	76.5726	534
	chr8:103,049,066-103,049,534	29.0425	469
	chr8:102,838,398-102,838,910	26.5179	513
	chr8:102,822,392-102,822,919	13.4375	528
	chr8:102,805,976-102,806,202	11.6241	227
PDE3B	chr11:14,621,513-14,622,267	24.9654	755
	chr11:14,622,401-14,623,083	12.3038	683
PLA1A	chr3:120,802,377-120,802,558	11.5989	182
PLA2G7	chr6:46,811,125-46,811,459	10.8366	335
SH3RF1	chr4:170,427,905-170,429,255	30.7452	1351
	chr4:170,377,325-170,377,452	10.7175	128
	chr4:170,272,975-170,273,177	10.1184	203
	chr4:170,261,789-170,262,253	26.2919	465
	chr4:170,250,579-170,250,860	13.09	282
TDRD1	chr10:115,928,777-115,929,226	42.7532	450
	chr10:115,929,474-115,929,753	17.2206	280
	chr10:115,931,749-115,931,952	12.9605	204
TMBIM1	chr2:218,845,599-218,846,084	15.9441	486
	chr2:218,842,616-218,843,563	68.8155	948
TMEM45B	chr11:129,190,576-129,191,309	26.0991	734
	chr11:129,192,367-129,192,815	16.6449	449
	chr11:129,227,301-129,227,768	16.9834	468
	chr11:129,228,731-129,229,530	28.771	800
ZNF385B	chr2:180,434,051-180,434,374	10.9614	324
	chr2:180,251,300-180,251,534	12.105	235
	chr2:180,250,103-180,250,510	19.5634	408